3
Dissociation Chemistry of 3-Oxetanone

3.1 INTRODUCTION

Small heterocyclic molecules play an important role as starting material in organic synthesis[Rotstein *et al.*, 2014; Bull *et al.*, 2016; Wuitschik *et al.*, 2006]. 3-oxetanone (1,3-epoxy-2-propanone, c$-C_3H_4O_2$) is one such example which is a highly strained molecule useful in ring expansion and addition reactions[Ruider *et al.*, 2013; Orr *et al.*, 2013; Ho and Aissa, 2012]. This molecule has also been proposed as a decomposition product of acetonylperoxy radical in the atmosphere[El-Nahas *et al.*, 2008]. A few electronic structure theory and spectroscopic studies focusing on the equilibrium properties such as geometry, ring puckering vibration, and non-bonded interactions, have been reported in the literature. Semiempirical[Combs and Rossie Jr, 1976] and *ab initio*[Thomson, 1982; Pasto *et al.*, 1982] calculations indicate a planar geometry with C_{2v} symmetry for this molecule (see Figure 3.1), which is consistent with infrared[Carreira and Lord, 1969; Durig *et al.*, 1970] and microwave[Gibson and Harris, 1972] spectroscopic predictions. Synchrotron based high resolution infrared investigations characterizing the ground state vibrational bands of 3-oxetanone molecule have been reported recently[Chen and van Wijngaarden, 2012b,a].

For the thermal decomposition of 3-oxetanone, two different modes of dissociation can be considered[Breuer *et al.*, 1975; Wright *et al.*, 2015] as shown in Figure 3.1. The first involves the formation of ketene + formaldehyde and the second one involves ethylene oxide + carbon monoxide formation. Photolysis of substituted 3-oxetanone with either methyl[Wagner *et al.*, 1966] or phenyl[Wasacz *et al.*, 1976] group leads to the formation of products similar to the ones shown for 3-oxetanone in Figure 3.1. Cyclobutanone, a four membered cyclic molecule similar to 3-oxetanone, forms analogous thermal dissociation products, cyclopropane (ethylene oxide in case of 3-oxetanone) + CO and ethylene + ketene.

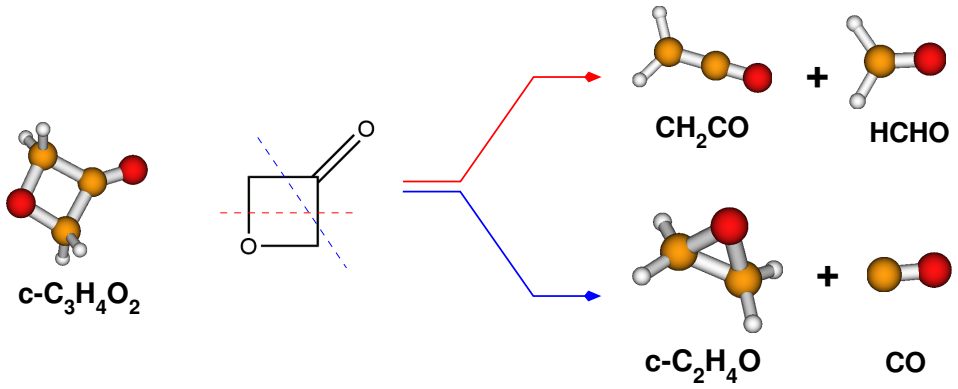

Figure 3.1 : Equilibrium geometry of 3-oxetanone molecule and the two considered thermal decomposition pathways forming ketene + formaldehyde and ethylene oxide + carbon monoxide.

Previous studies[Mcgee and Schleifer, 1972; Das *et al.*, 1954; Braun *et al.*, 1984] on cyclobutanone molecule have shown that cyclopropane channel requires greater activation energy compared to the ketene channel. In addition, Rice-Ramsperger-Kassel-Marcus (RRKM) theory[Marcus and Rice, 1951; Marcus, 1952; Rosenstock *et al.*, 1952] calculations have predicted that the reaction rate of the cyclopropane channel would be ~2 orders of magnitude slower compared to the ketene channel[Breuer *et al.*, 1975].

Only a limited number of studies on the decomposition of 3-Oxetanone are present in the literature. Almost four decades ago, an article was published[Breuer *et al.*, 1975] in which unimolecular decomposition rate of 3-oxetanone was investigated using RRKM theory. In that work, only the ketene pathway was considered, and the activation energy was similar to that of cyclobutanone. Another route leading to ethylene oxide and carbon monoxide was not considered due to the low reaction rate for similar pathway in cyclobutanone. Recently, pyrolysis products of 3-oxetanone in gas phase were investigated by Fourier transform infrared spectroscopy and photo-ionization mass spectrometry techniques[Wright *et al.*, 2015]. In these experiments, new reaction products were identified such as ethylene and methyl radicals along with the above mentioned products such as ketene, formaldehyde, ethylene oxide, and carbon monoxide. However, branching ratios between two primary dissociation pathways and quantitative analysis of CO as a reaction product were not possible in that study.

Gas phase dissociation chemistry of 3-oxetanone was investigated in the present work using electronic structure theory, direct dynamics simulations, [Sun and Hase, 2003; Paranjothy *et al.*, 2013] and RRKM rate constant calculations. Characterization of energy profile of the dissociation pathways of 3-oxetanone was done using different levels of electronic structure theory. Density functional B3LYP/6-31G* level of theory was used for direct dynamics calculations. The aim is to characterize the complete reaction energy profile of decomposition of 3-oxetanone, study the reaction mechanisms at the atomic level, and to compute branching ratios. Besides the previously known dissociation channels shown in Figure 3.1, a new pathway invoking ring opened isomer of ethylene oxide isomer was found in the simulations. Electronic structure calculations predict that the energy barrier for this new dominant separation channel is lowest among all pathways.

3.2 POTENTIAL ENERGY SURFACE

All stationary points of the two main dissociation pathways of 3-oxetanone molecule shown in Figure 3.1, were characterized using different levels of electronic structure theory. Energies of reactant, products, and the corresponding transition states are summarized in Table 3.1. Electronic energies reported in the table are not zero-point energy corrected. Single-point energy calculations at CCSD(T)/6-311G* level using MP2 optimized geometries were used as benchmark calculations. The optimized geometries of all the stationary points were identified by calculating their normal mode frequencies. All the minima had 3N-6 real vibrational frequencies whereas transition states had one imaginary vibrational frequency. To confirm optimized transition states connect the right product to the reactant, intrinsic reaction coordinate (IRC) calculations were performed.

Table 3.1 : Energies of stationary points on the 3-oxetanone dissociation pathways shown in Figure 3.1. Numbers are in units of kcal/mol and are relative to the reactant energy at a given level of theory.

theory	c$-C_3H_4O_2$	ts1[a]	CH_2CO+HCHO	ts2[b]	c$-C_2H_4O+CO$
B3LYP/6-31G*[c]	0.0	58.6	10.1	95.9	12.4
B3LYP/6-311G*	0.0	57.2	4.2	94.8	8.5
M06-2X/6-31G*	0.0	69.7	15.9	96.6	8.8
M06-2X/6-311G*	0.0	68.4	11.1	95.3	5.5
PBE0/6-31G*	0.0	64.0	18.8	97.6	17.1
PBE0/6-311G*	0.0	63.0	14.2	96.7	14.9
MP2/6-31G*	0.0	73.6	10.4	100.0	4.8
MP2/6-311G*	0.0	73.4	6.6	97.1	2.7
CCSD(T)/6-31G*[d]	0.0	52.1	10.5	98.9	4.4
CCSD(T)/6-311G*[d]	0.0	51.6	7.3	95.8	2.2

[a] Transition state for the ketene pathway
[b] Transition state for the ethylene oxide pathway
[c] Direct dynamics calculations were performed at this level of theory
[d] CCSD(T) energies computed by single point calculations using the corresponding MP2 optimized geometries

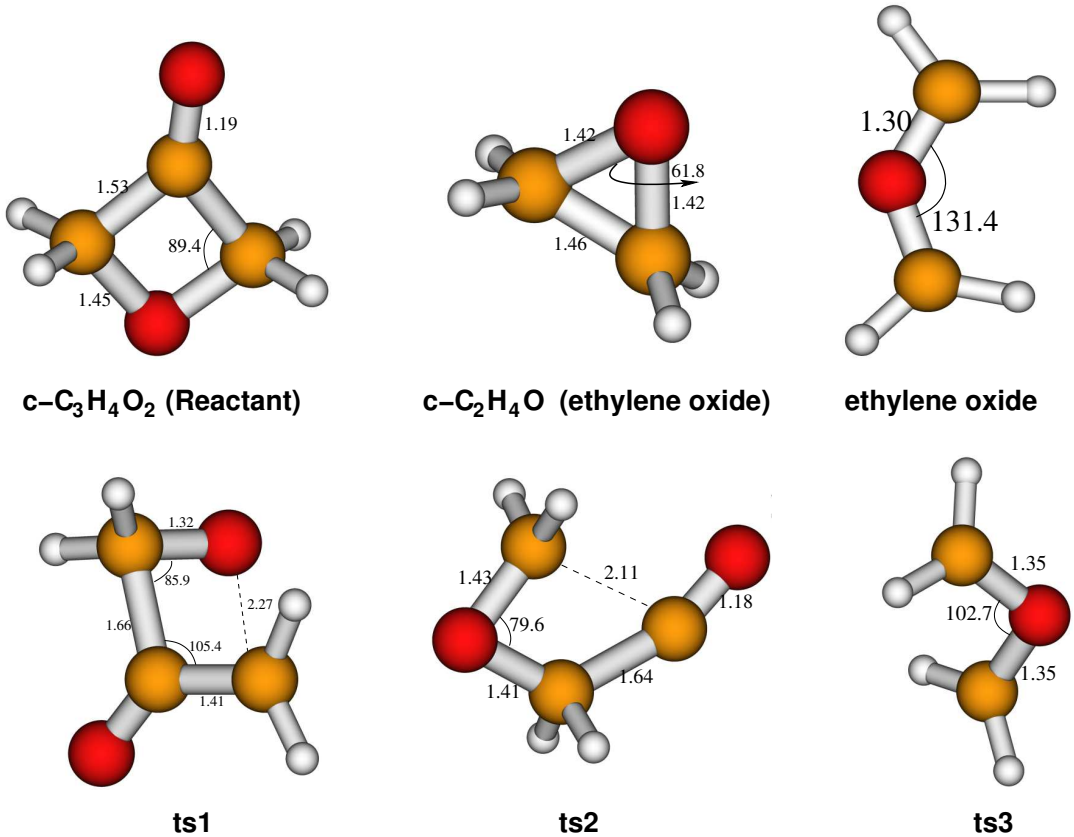

Figure 3.2 : Optimized geometries at B3LYP/6-31G*, bond angle values are in degree (°) and bond lengths in angstroms (Å).

All the calculations show that both the dissociation channels are endoergic in nature, and ketene pathway has lower barrier compared to ethylene oxide pathway. Barrier heights for ketene and ethylene oxide channels range from 51.6 to 73.6 kcal/mol and 94.8 to 100.0 kcal/mol, respectively. In comparison to the CCSD(T) benchmark calculation, MP2 method overestimates the reaction barrier, although the overall reaction energy agrees with the benchmark values. The hybrid density functional B3LYP method using 6-31G* and 6-311G* basis sets predict barrier heights near to CCSD(T) values. The direct dynamics simulations were performed at the B3LYP/6-31G* level of theory due to accuracy and the lower computational time requirements for this method.

Potential energy profile for dissociation pathways of 3-oxetanone computed at the B3LYP/6-31G* level of theory are shown in Figure 3.3 and optimized geometries of the reactant, and transition states are shown in Figure 3.2 along with bond lengths and bond angles. Bond angle values are in degree (°) and bond lengths in angstroms (Å).

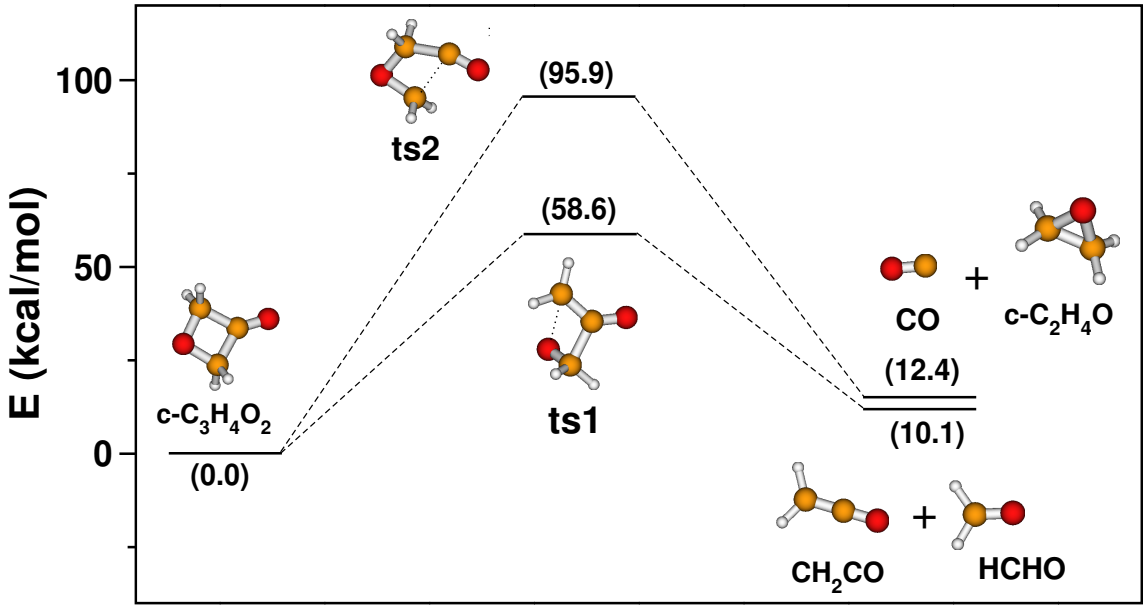

Figure 3.3 : Potential energy profile of 3-oxetanone dissociation pathways computed at the B3LYP/6-31G* level of theory. The numbers in bracket are energies in kcal/mol relative to the reactant 3-oxetanone molecule. The corresponding optimized geometries are also shown.

ts1 which connects the reactant to ketene product is non-planar and ts2 connecting ethylene oxide is planar. The reference CCSD(T) calculations show that ketene pathway has much lower barrier than ethylene oxide channel. It can be seen from Table 3.1 that at the CCSD(T)/6-31G* level, ethylene oxide pathway exhibits a barrier height of 98.9 kcal/mol as compared to 52.1 kcal/mol for the ketene pathway. Similarly at CCSD(T)/6-311G* level, barrier values are 95.8 kcal/mol and 51.6 kcal/mol for the ethylene oxide and ketene channels, respectively. It is important to note that in the dissociation of cyclobutanone, the cyclopropane channel which is similar to ethylene oxide pathway in 3-oxetanone has much higher energy barrier in comparison to the other ketene channel[Braun *et al.*, 1984]. This leads to lower reaction rate for the cyclopropane channel, predicted by RRKM theory[Breuer *et al.*, 1975]. Therefore, the ketene route is expected to become the dominant decomposition pathway in the thermal decomposition of 3-oxetanone.

Potential energy surface provides some idea of molecular reactivity, but actual dynamics may show variations from the predictions made by electronic structure theory. In order to understand the complete reaction mechanisms and the branching ratio of products obtained by dissociation of 3-oxetanone, Born-Oppenheimer direct dynamics simulations[Sun and Hase, 2003; Paranjothy *et al.*, 2013] were performed at the B3LYP/6-31G* level of theory. For the trajectory initial conditions, classical micro-canonical sampling technique[Hase and Buckowski, 1980; Peslherbe *et al.*, 1999] was used. Simulations were performed at three different energies, viz., E_{tot} = 150, 200 and 300 kcal/mol. A total of 150 trajectories at each total energy (amounting to 450 trajectories) were generated. Due to high ring strain, 3-oxetanone molecule is expected to have high reactivity and hence the trajectories were integrated only up-to 3 ps with a step-size of 1 fs. The classical equations of motion were integrated using the symplectic integrator of sixth-order[Schlier and Seiter, 1998, 2000]. Although this integrator is computationally expensive compared to others such as [Swope *et al.*, 1982]velocity Verlet (3rd-order integrator), it provided very good energy conservation in all the trajectories. Classical trajectories were calculated by a tight coupling algorithm[Lourderaj *et al.*, 2014] interfacing VENUS[Hase *et al.*, 1996; Hu *et al.*, 1991] with NWChem[Valiev *et al.*, 2010]. The default values of the convergence criteria provided in the NWChem program were used in all the calculations. On a Lenovo 10 core workstation, it required approximately 48 hours of calculation time to integrate a trajectory to 3 ps.

3.3 DIRECT DYNAMICS

At each excitation energy, E_{tot} = 150, 200, and 300 kcal/mol, a total of 150 trajectories were generated, resulting in a total of 450 trajectories. In all the trajectories, total energy was conserved within $E_{tot} \pm 0.5$ kcal/mol. The energy conservation plots (E_{tot} as a function of time) for few sample trajectories are shown in Figure 3.4.

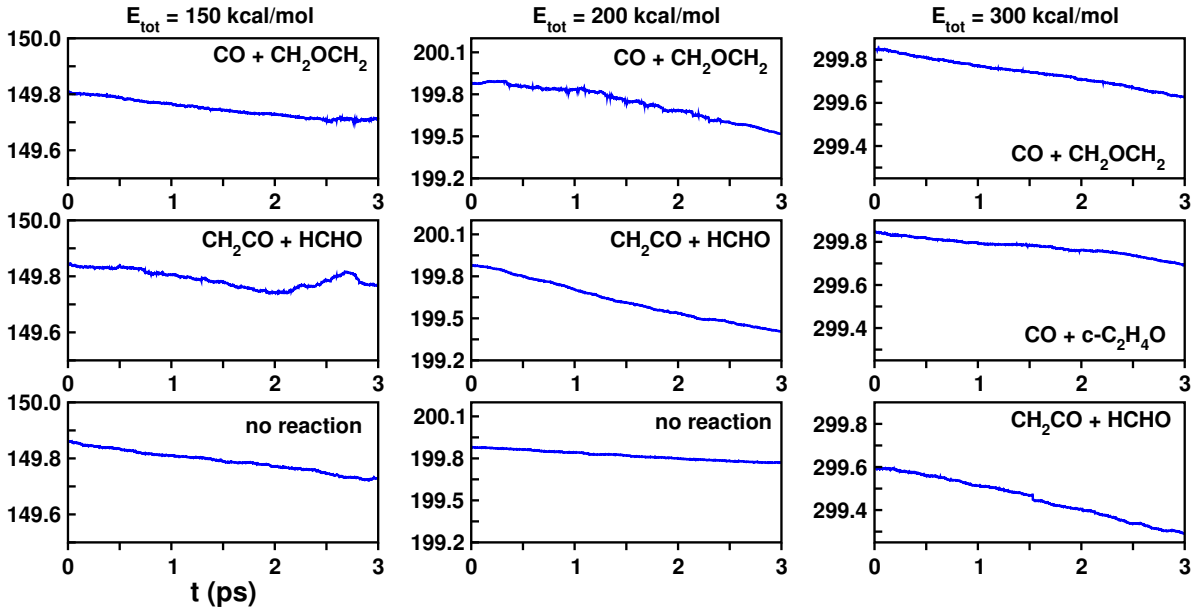

Figure 3.4 : Total energy as a function of time for a few sample classical trajectories. First, second, and third columns correspond to E_{tot} = 150, 200, and 300 kcal/mol, respectively. Trajectory outcomes (reaction products) are shown inside the plots. In all plots, x-axes ranges are same.

The trajectories were animated to establish reaction mechanisms at the atomic level and calculate branching ratios among possible reaction pathways. All the 150 trajectories showed dissociation at the highest total energy 300 kcal/mol, whereas 147 and 59 trajectories, were reactive at E_{tot} = 200 and 150 kcal/mol, respectively. Total reactivity was 100, 98 and 39 % at 300, 200 and 150 kcal/mol, respectively. Many dissociation patterns were observed, and trajectory events are summarized in Table 3.2.

Table 3.2 : Overall trajectory events following excitation of the 3-oxetanone molecule

pathway	150[a]	200[a]	300[a]
$CH_2CO + HCHO$	1	29	38
$c-C_2H_4O + CO$	0	0	9
CH_2OCH_2[b] + CO	57	107	75
minor pathways	1	11	28
no reaction[c]	91	3	0
total	150	150	150

[a] Excitation energy E_{tot} in kcal/mol. A total of 150 trajectories were generated for each energy
[b] Ring opened isomer of ethylene oxide
[c] Trajectories that did not dissociate during the entire integration time of 3 ps

3.3.1 Ketene Channel: $CH_2CO + HCHO$

As it is clear from Figure 3.3, the ketene route has a smaller activation barrier (58.6 kcal/mol) in comparison to the ethylene oxide pathway (95.9 kcal/mol). In the simulations, 1, 29, and 38 trajectories followed this pathway to dissociate into CH_2CO + HCHO at E_{tot} = 150, 200, and 300 kcal/mol, respectively. This ketene channel was observed in previous pyrolysis experiments[Wright *et al.*, 2015]. Although, having the lower reaction barrier, the fraction of trajectories dissociated via this channel is less. Further dissociation of CH_2CO into $CH_2 + CO$ was observed at only the highest energy simulation (300 kcal/mol). Out of the total 38 trajectories following the ketene channel, 24 trajectories showed further dissociation into CH_2 + CO. None of the trajectories showed subsequent dissociation of CH_2CO in the 200 and 150 kcal/mol simulations. Summary of subsequent products of ketene channel is presented in Table 3.3.

The energy profile for $CH_2CO \longrightarrow CH_2 + CO$ reaction is shown in Figure 3.5(d) and it has no transition state. The endoergicity of the reaction is 101.5 kcal/mol computed at the B3LYP/6-31G* theory. In a previous study,[Klippenstein *et al.*, 1996; Xiao *et al.*, 2013] it was reported that dissociation of ketene in the singlet state is barrier-less and endoergic. This reaction was not observed at lower energies (150 and 200 kcal/mol) due to less available energy. Thermal dissociation of ketene using Shock tube experiments have been reported earlier[Hidaka *et al.*, 1994; Tsuda and Kuratani, 1968] and these studies have indicated high stability for ketene. These experiments have shown that temperatures above 1300°C are required for further dissociation of ketene. Consistently, only at the highest energy simulation, dissociation of ketene was observed. An important point to be noted here is that CO formation can occur via ethylene oxide pathway directly as well as via subsequent dissociation of ketene. Snapshots of a typical trajectory showing this pathway are given in Figure 3.6(a).

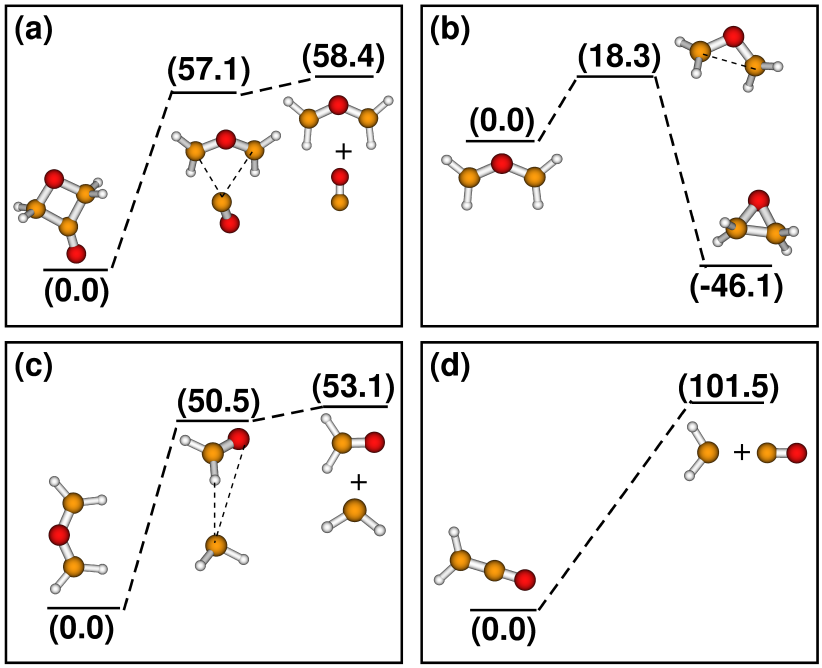

Figure 3.5 : Potential energy profiles for (a) 3-oxetanone dissociating to CH_2OCH_2 + CO (b) isomerization of CH_2OCH_2 to ethylene oxide (c) dissociation of CH_2OCH_2 to HCHO + CH_2 and (d) ketene dissociation to CH_2 + CO. The numbers in brackets are energies in kcal/mol, relative to the corresponding reactants.

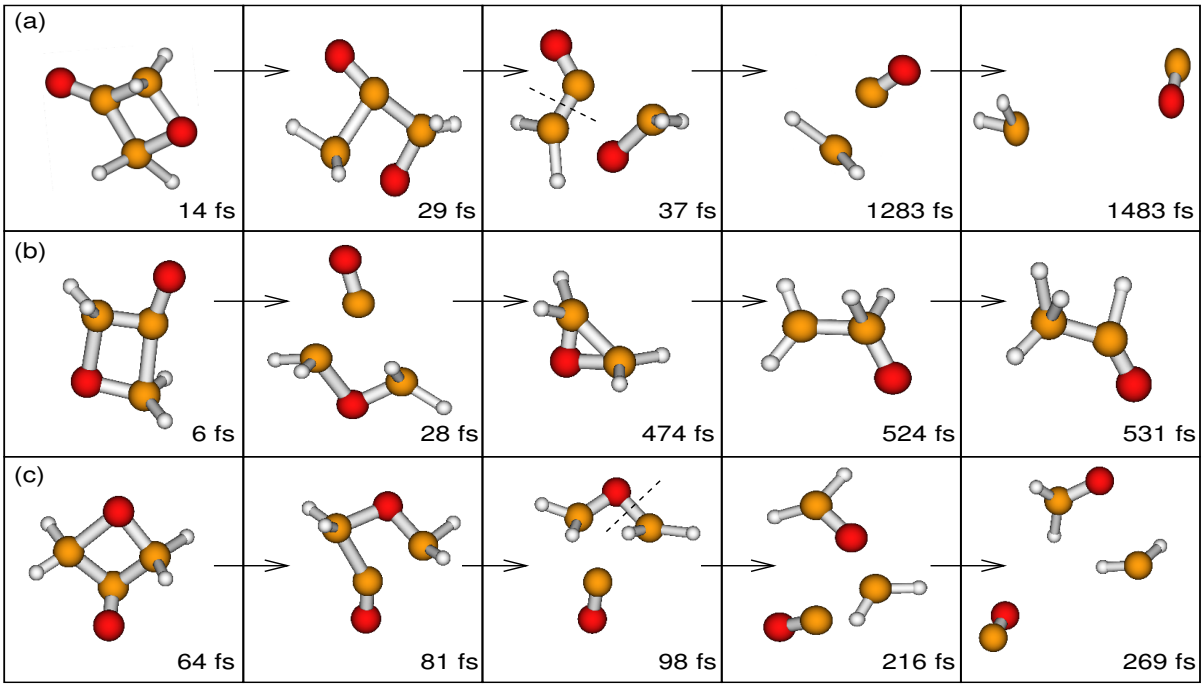

Figure 3.6 : Snapshots of trajectories showing dissociation of 3-oxetanone to (a) $HCHO + CH_2CO \longrightarrow HCHO + CH_2 + CO$ (b) $CO + CH_2OCH_2 \longrightarrow CO + c{-}C_2H_4O \longrightarrow CO + CH_3CHO$ and (c) $CO + CH_2OCH_2 \longrightarrow CO + CH_2 + HCHO$.

It can be seen from Figure 3.6(a) that dissociation of 3-oxetanone to form $CH_2CO + HCHO$ occurs around 30 fs. Further dissociation of ketene happened after 1 ps to form CH_2 + CO. In many trajectories much higher lifetime of ketene was found indicating stability. None of the trajectories showed subsequent reactions of HCHO.

3.3.2 Ethylene Oxide Channel: $c-C_2H_4O$ + CO

Only at the highest energy E_{tot} = 300 kcal/mol, 9 trajectories followed the high activation energy pathway to form ethylene oxide and CO. Such a small fraction is expected due to the high energy barrier associated with this pathway. None of the trajectories at 150 and 200 kcal/mol showed dissociation via this pathway (see Table 3.2). Note that there is strong evidence present in literature[Wright *et al.*, 2015] suggesting the formation of ethylene oxide from 3-oxetanone. Subsequent dissociation of ethylene oxide was observed in the simulation resulting in products such as HCHO, CO, CH_2, CH_2CO(ketene), and H_2. In the thermal decomposition of 3-oxetanone, ketene formation from ethylene oxide was suspected in the experiments[Wright *et al.*, 2015] but could not be confirmed. Out of the 9 trajectories following the ethylene oxide path at 300 kcal/mol, 3 trajectories showed further dissociation to form ketene + H_2 as products. Also, in 5 trajectories ethylene oxide further dissociated into HCHO + CH_2 + CO whereas one into 2 CO + H_2 + CH_2 (see Table 3.3). These are indirect pathways giving the same products as observed in the primary ketene channel.

In addition to the trajectories described above to form ethylene oxide, there are several other trajectories which did not follow the highest activation energy route, but gave the same product shown in Figure 3.3. In this new pathway, 3-oxetanone dissociates first into a ring-opened isomer of ethylene oxide, which further isomerizes to cyclic ethylene oxide or further dissociates. This route was dominant in the simulations to form ethylene oxide as a product. This new pathway to form ethylene oxide was not considered before in the literature.

Table 3.3 : Various different dissociation pathways observed for the 3-oxetanone molecule

pathway	150[a]	200[a]	300[a]
$CH_2CO + HCHO$	1	29	14
$CH_2CO + HCHO \longrightarrow CH_2 + CO + HCHO$	0	0	24
$CO + c-C_2H_4O \longrightarrow CO + HCHO + CH_2$	0	0	5
$CO + c-C_2H_4O \longrightarrow CO + H_2 + CH_2CO$	0	0	3
$CO + c-C_2H_4O \longrightarrow 2CO + H_2 + CH_2$	0	0	1
$CO + CH_2OCH_2$	46	9	0
$CO + CH_2OCH_2 \longrightarrow CO + CH_2 + HCHO$	0	44	55
$CO + CH_2OCH_2 \longrightarrow CO + c-C_2H_4O$	11	47	0
$CO + CH_2OCH_2 \longrightarrow CO + c-C_2H_4O \longrightarrow CO + CH_3CHO$[b]	0	5	7

[a] Excitation energy E_{tot} in kcal/mol

[b] CH_3CHO underwent further dissociation to form CO, CH_4, etc.

3.3.3 CH_2OCH_2 + CO Channel

This is a new route observed in the simulations to form CO + ethylene oxide (see Table 3.2). It was considered that 3-oxetanone can dissociate into ketene + HCHO and ethylene oxide ($c-C_2H_4O$) + CO, with the latter one requiring high activation energy. So, the ketene pathway should have been dominant purely from an energetic point of view. But in the direct dynamics simulations, ethylene oxide + CO was observed as dominant products. The reason behind the

formation of ethylene oxide + CO as major products rather than the lower energy ketene products is that 3-oxetanone molecule followed a new route to form same product. This new pathway involves the formation of ring opened isomer of ethylene oxide (CH_2OCH_2) + CO, which further isomerizes to c$-C_2H_4O$ + CO as final products (see Table 3.3). This ring-opened isomer is planar with C_{2v} symmetry and is much less stable[Wesdemiotis *et al.*, 1990; Belbruno, 1997; Yang *et al.*, 2007], and isomerizes to the more stable (by 46.1 kcal/mol computed at B3LYP/6-31G*) ethylene oxide. Ketene products are more stable than c$-C_2H_4O$ + CO which makes this pathway to be thermodynamically controlled whereas new ethylene oxide pathway has more stable TS than ketene pathway, so it is kinetically preferable. A total of 57, 107 and 75 trajectories followed this new pathway at E_{tot} = 150, 200, and 300 kcal/mol, respectively. The energy profile for this reaction calculated at B3LYP/6-31G* level is shown in Figure 3.5(a). Energy profile is nearly flat with transition state and product lie very close to each other, which is 57.1 and 58.4 kcal/mol, respectively. The reason for the less stability of product is the presence of free radical on the C-atoms. Since, activation energy for this route is lowest among all possible dissociation pathways, this is energetically most favorable. Subsequent dissociation of CH_2OCH_2 happened to give many different products (see Table 3.3). At the highest energy, all the 75 trajectories showed further dissociation, whereas 11 (out of 57) and 98 (out of 107) trajectories at 150 and 200 kcal/mol, respectively, underwent subsequent reactions. All possible subsequent reactions can be seen in Table 3.3, among which two were major. One is the isomerization to cyclic ethylene oxide and other is dissociation to HCHO + CH_2. The energy profile for ring closing of CH_2OCH_2 to form ethylene oxide is shown in Figure 3.5(b), which requires an energy barrier[Belbruno, 1997] of 18.3 kcal/mol via a counter-rotatory transition state. In the analysis of simulation results, it was found that 11, 52 and 7 trajectories showed isomerization at E_{tot} = 150, 200, and 300 kcal/mol, respectively. This shows that this route is the main source of ethylene oxide formation observed in experiments[Wright *et al.*, 2015]. Snapshots of an example trajectory following this route are represented in Figure 3.7(a).

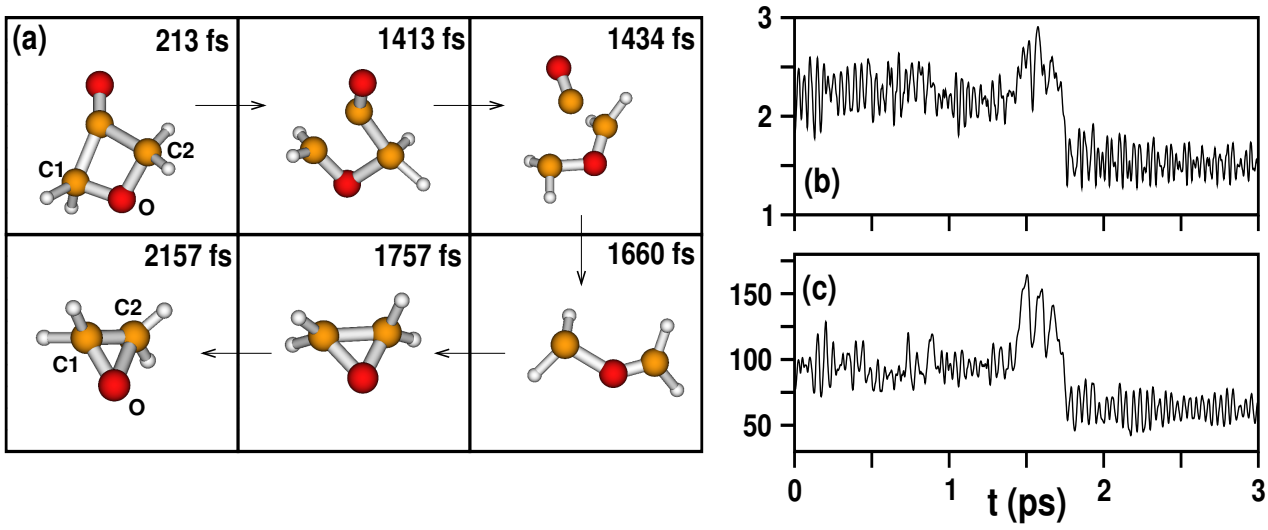

Figure 3.7 : (a) Snapshots of a typical trajectory showing dissociation of 3-oxetanone to CO and CH_2OCH_2 which isomerizes to ethylene oxide (b) C_1-C_2 distance (in Å) (c) $\angle C_1-O-C_2$ angle (in degree) as a function of time. Isomerization of CH_2OCH_2 to ethylene oxide happens around 1700 fs.

Bond distance C1-C2 (in Å) and $\angle C_1-O-C_2$ angle (in degree) corresponding to the shown trajectory are given in Figures 3.7(b) and (c), respectively. It can be seen from Figure 3.7(a)

that separation of 3-oxetanone to CH_2OCH_2 occurs around 1400 fs and the isomerization to ring-closed form at 1700 fs. Optimized geometry of CH_2OCH_2 and cyclic ethylene oxide are shown in Figure 3.8. The C1-C2 bond distance and $\angle C_1-O-C_2$ angle values are 1.46 Å and 61.8°, respectively, for cyclic ethylene oxide (see in Figure 3.8). In Figure 3.7(b) it can be clearly seen that C1-C2 bond distance reaches to the equilibrium value 2.38 Å and then decreases to 1.46 Å (equilibrium bond distance of cyclic ethylene oxide). Similarly $\angle C_1-O-C_2$ angle reaches to maximum bond angle 131.4° at around 1660 fs, and then decreases to 61.8°. Both Figures Figure 3.7(b) and (c), clearly establish the formation of ethylene oxide via the new pathway.

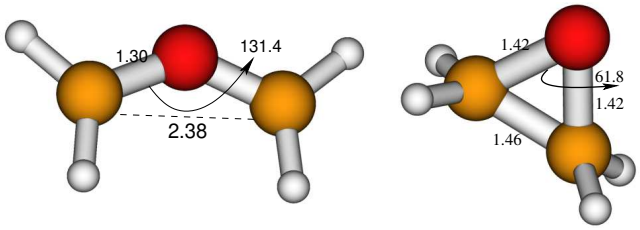

Figure 3.8 : Optimized geometries of two isomers of ethylene oxide at B3LYP/6-31G* level

In a very small number of trajectories (a total of 12), ethylene oxide molecule showed [1,2]-H shift to form acetaldehyde. Acetaldehyde was suspected to be an intermediate in the pyrolysis experiments of 3-oxetanone, but was not confirmed[Wright *et al.*, 2015]. This requires high activation energy[Yang *et al.*, 2007], so observed in a very small fraction of trajectories. Snapshots of an example trajectory showing the formation of acetaldehyde are presented in Figure 3.6(b). 3-oxetanone molecule first forms the ring-opened CH_2OCH_2 isomer around 28 fs and then it isomerizes to cyclic ethylene oxide. This cyclic ethylene oxide again undergoes ring opening and [1,2]-H shift happens to form acetaldehyde at around 530 fs. Another major subsequent reaction of CH_2OCH_2 species is the formation of HCHO +CH_2. This reaction was seen in 44 and 55 trajectories at E_{tot} = 200 and 300 kcal/mol energy, respectively, and might be a major source of formaldehyde formation observed in the experiments[Wright *et al.*, 2015] along with the primary dissociation pathway i.e. the ketene channel. At 150 kcal/mol, none of the trajectories followed this route, indicating this is a high energy pathway. Figure 3.6(c) shows trajectory snapshots of an example trajectory forming HCHO + CH_2 seen in the 98 fs frame. The reaction energy profile of this pathway is shown in Figure 3.5(c), which is an endoergic reaction with a barrier height of 50.5 kcal/mol.

Among the subsequent reactions of CH_2OCH_2, dissociation reactions have larger reaction barriers than the isomerization reactions. This is the reason why isomerization was observed at low energy conditions whereas dissociations dominate at high energies. Calculated values of activation energy are higher than the values reported earlier[Yang *et al.*, 2007] at CCSD(T)/cc-pVTZ//B3LYP/6-311++G(d,p) (38.8 kcal/mol for separation and 10.9 kcal/mol for isomerization) level, but qualitatively similar. In a previous work,[Yang *et al.*, 2007] few other isomerization/dissociation reactions of CH_2OCH_2 molecule were reported resulting in CH_3OCH, CHOH, etc., but these are energetically not favorable and not observed in the present dynamics simulations.

3.3.4 Minor Pathways

In addition to the above described major pathways, there are few minor dissociation channels observed in the simulations. A total of 40 out of 450 trajectories followed these pathways and a summary is given in Table 3.4. These minor channels were observed primarily at 200 and 300 kcal/mol simulations.

Table 3.4 : Minor pathways observed in the dissociation of 3-oxetanone

product	ΔE^a	200[b]	300[b]
$H_2 + c{-}COCH_2CO$[c]	83.2	1	8
CH_3COCHO[d]	-15.8	1	4
$CH_2 + CHOCHO$[e]	105.8	0	4
$H_2 + CO + CHCOH$	62.2	0	3
$CO + CH_2CHOH$[f]	0.2	0	2
$CHOCH_2CHO$	-15.5	3	0

[a] $\Delta E = E_{product} - E_{3\text{-oxetanone}}$ (in kcal/mol)
[b] Excitation energy in kcal/mol
[c] Further dissociated to CH_2CO, CH_2, and CO
[d] Further dissociated to CH_2CO, CH_2, CH_3, CH_4, CHO, and CO
[e] Further dissociated to HCHO, CH_2, H_2, and CO
[f] Further dissociated to H_2O and C_2H_2

The six pathways listed in the above table are observed as minor pathways. Five and four trajectories dissociated to CH_3COCHO and CH_2 + CHOCHO (glyoxal), respectively. Further fragmentation of these products happened due to availability of high energy into CH_2CO, CH_2, CH_3, CH_4, CHO, CO, HCHO, and H_2. Isomerization of 3-oxetanone to ring-opened forms such as CH_3COCHO (2-oxopropanal) and $CHOCH_2CHO$ (propanedial) are exoergic in nature owing to the ring strain in the molecule. Nine trajectories showed dehydrogenation reaction to give cyclic $c{-}COCH_2CO$, which further dissociated to CH_2CO, CH_2, and CO. Four, three, and two trajectories dissociated into CH_2 + CHOCHO (glyoxal), H_2 + CO + CHCOH, and CO + CH_2CHOH (vinyl alcohol), respectively. These pathways are endoergic in nature. Equilibrium geometries of all these species were computed at the same B3LYP/6-31G* level of theory and shown in Figure 3.9.

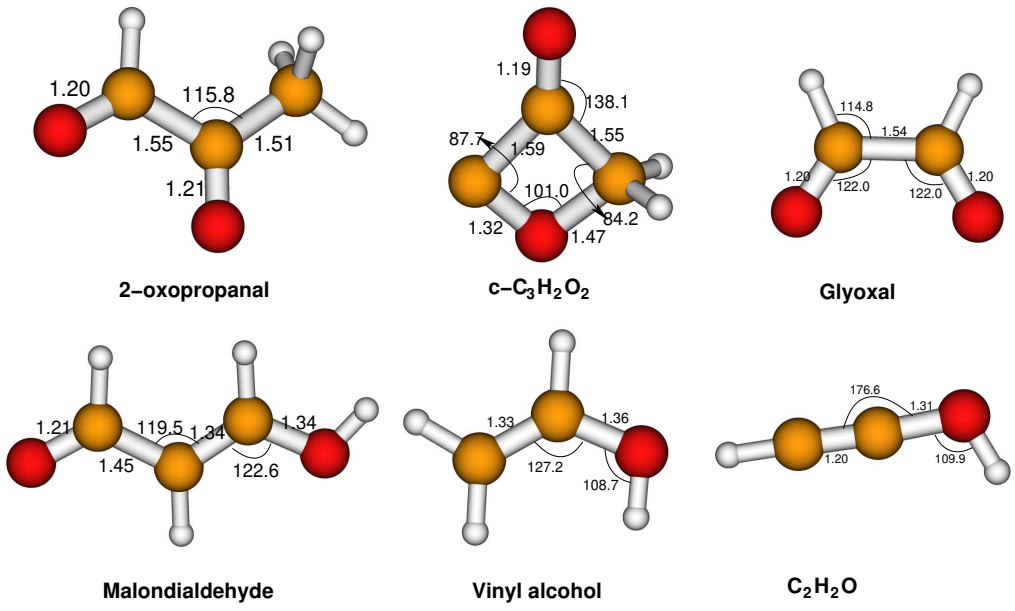

Figure 3.9 : Optimized geometries at B3LYP/6-31G*, bond angle values are in degree (°) and bond lengths in angstroms (Å).

Snapshots of trajectories wherein 3-oxetanone dissociates via minor pathways are shown in Figure 3.10.

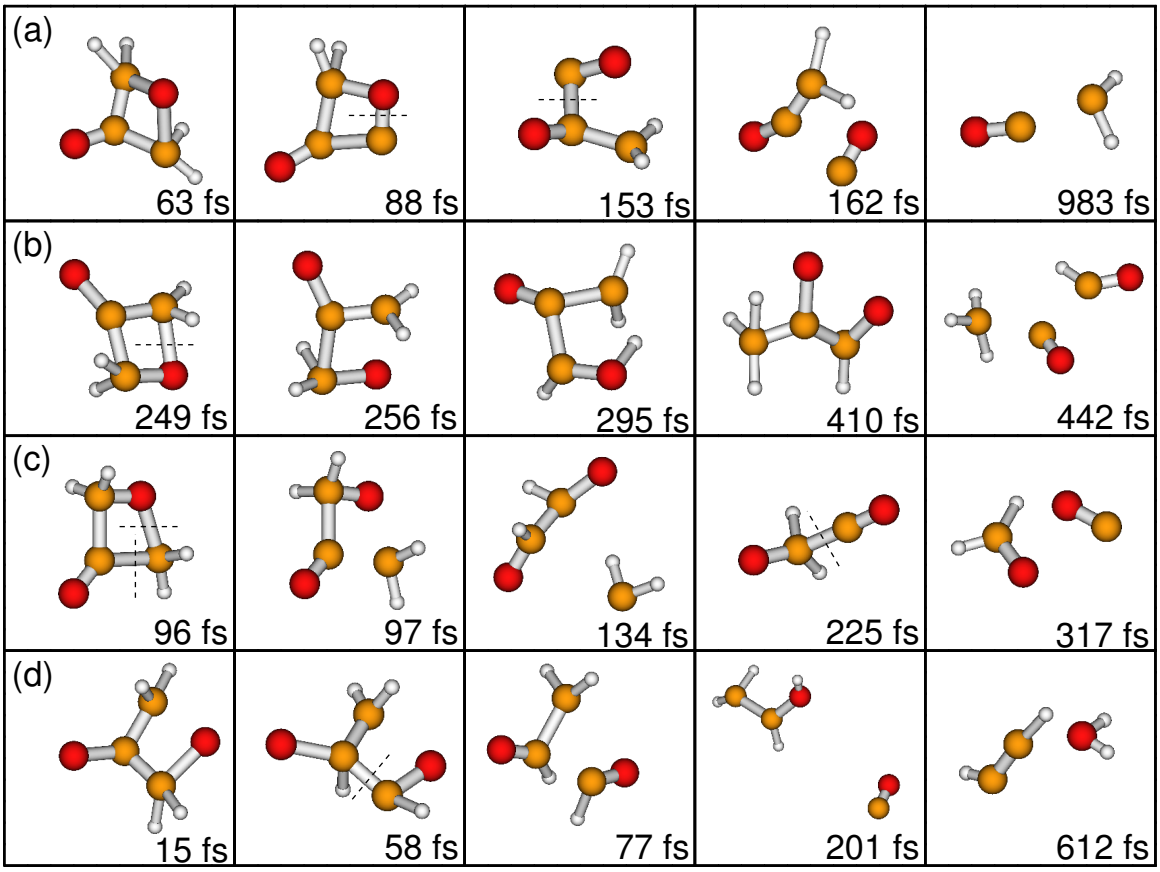

Figure 3.10 : Snapshots of a typical trajectory showing dissociation of (a) $c-C_3H_4O_2 \longrightarrow H_2 + c-COCH_2CO \longrightarrow H_2 + CO + CH_2CO \longrightarrow H_2 + 2CO + CH_2$ (b) $c-C_3H_4O_2 \longrightarrow CH_3COCHO \longrightarrow CH_3 + CO + CHO$ (c) $c-C_3H_4O_2 \longrightarrow CH_2 + CHOCHO \longrightarrow CH_2 + CO + HCHO$ (d) $c-C_3H_4O_2 \longrightarrow CO + CH_2CHOH \longrightarrow CO + H_2O + C_2H_2$

Further fragmentation of these species were also observed forming CH_2CO, CO, and HCHO etc., with the exception of CHCOH. Formation of vinyl alcohol was observed in two trajectories which later dehydrated to form acetylene. Experiments[Wright *et al.*, 2015] could not detect such small fraction of water or acetylene in the pyrolysis of 3-oxetanone. Note that some of these minor pathways yielded the same products as obtained in primary pathways discussed above.

3.3.5 Elimination of CO from 3-Oxetanone

An interesting question about the gas phase dissociation of 3-oxetanone that could not be answered in the experiments[Wright *et al.*, 2015] is the amount of CO that was produced by direct dissociation of 3-oxetanone and the secondary dissociation of the primary products, i.e. the quantification of CO production. This question can be answered from the present simulation results. Among the earlier mentioned two major dissociation channels of 3-oxetanone, ethylene oxide channel is a direct source of CO elimination. But the results of the simulation show that, in

addition to the direct route mentioned above, further decomposition of ketene and other small decomposition channels also lead to formation of CO. Figure 3.11(a) gives the fraction of CO elimination trajectories forming through primary and secondary pathways. As can be seen from figure, the amount of CO formation increases with the total available energy, and CO elimination occurs through secondary channels when the energy is sufficiently high.

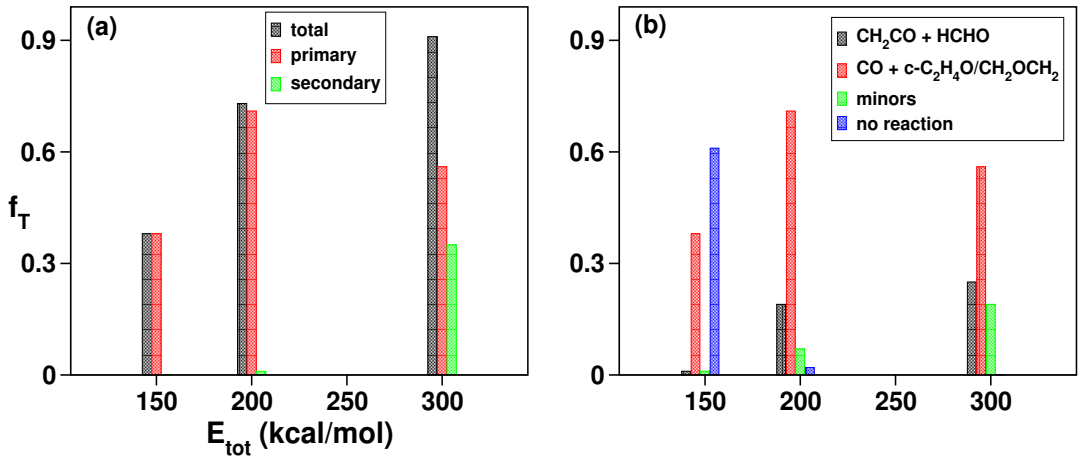

Figure 3.11 : Fraction of trajectories f_T as a function of E_{tot} showing (a) CO elimination via primary dissociation of 3-oxetanone (red), secondary decomposition of reaction products (green), and the total amount of trajectories eliminating CO (black) (b) the branching of 3-oxetanone dissociation products into various different pathways.

3.3.6 RRKM Calculations

The ketene dissociation channel of 3-oxetanone was studied by RRKM theory in an earlier work[Breuer *et al.*, 1975]. The energy barrier of analogous cyclobutanone molecule was used to calculate the rate constant, since there were no detailed electronic structure data on the dissociation pathways of 3-oxetanone were available. In the present work, RRKM rate constants (k_{RRKM}) for the dissociation channels of 3-oxetanone were calculated using electronic structure data at the B3LYP/6-31G* level. The calculations were done using Beyer−Swinehart direct count algorithm[Zhu and Hase, 1994; Beyer and Swinehart, 1973] and classical barrier heights (without zero point energy corrections) for the dissociation channels were used.

The graph plotted in Figure 3.12 shows k_{RRKM} values for the pathways forming ketene + formaldehyde, ethylene oxide + CO and CH_2OCH_2 + CO as a function of total energy. It can be clearly seen that rate constant for the CH_2OCH_2 channel is the maximum among all three. The rate constants for the ethylene oxide channel has the smallest value at lower energy initial conditions and increases as the available energy increases. The smallest rate constant value for c−C_2H_4O + CO channel can be understood due to high potential barrier for the reaction. Rate constants for the ketene channel are intermediate among all three possible pathways, but at larger energy value ethylene oxide channel becomes larger than those for the ketene pathway. The results of the simulations, summarized in 3.2, are qualitatively consistent with the RRKM theory predictions.

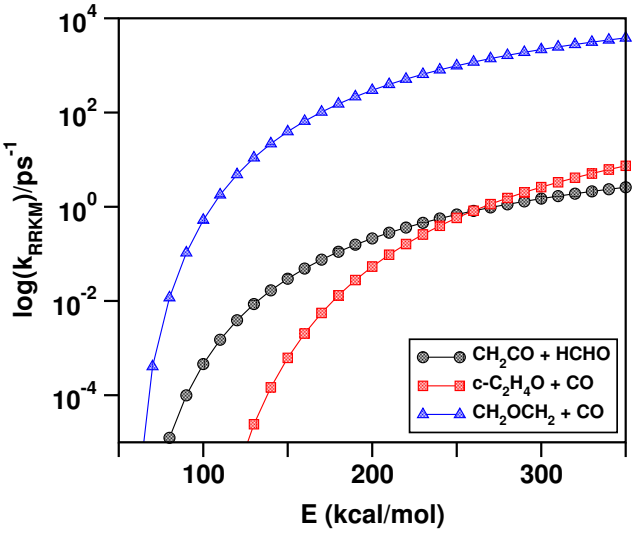

Figure 3.12 : RRKM theory rate constants k_{RRKM} as a function of energy for the dissociation pathways of 3-oxetanone.

3.4 SUMMARY

The gas phase decomposition of 3-oxetanone molecule was studied using electronic structure theory calculations, direct dynamics simulations, and RRKM theory. It was reported in the earlier studies that two main dissociation channels for this molecule are ketene + formaldehyde and ethylenoxide ($c-C_2H_4O$) + carbon monoxide. The results of the electronic structure calculations show that both the pathways are endoergic in nature, and the ethylene oxide pathway has a greater potential energy barrier than the ketene pathway. To understand the actual reaction mechanisms, direct classical trajectory simulations were performed at the B3LYP/6-31g* level of theory. Classical micro-canonical sampling technique was used to do the dynamical simulations. A total of 150 trajectories were generated at 150, 200 and 300 kcal/mol energies. Due to high potential energy barrier for ethylene oxide channel, it is expected to be a minor pathway compared to ketene channel, and the simulations showed the same behavior.

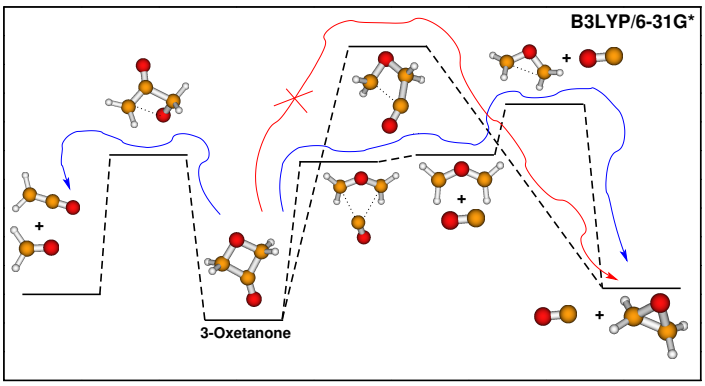

In addition to the reported two primary pathways, a new pathway was found in the simulations involving CO and ring-opened isomer of ethylene oxide, which later isomerized to ethylene oxide or underwent further dissociation. This new pathway has the lowest potential energy barrier, so a major fraction of trajectories preferred this channel. Comparative analysis of

all the three pathways along with possible minor pathways has been summarized in Figure 3.11(b). As one can see, ketene channel was less preferred at all three energy values in comparison to ethylene oxide + CO channel. Ketene channel was considered as dominant one in previous studies[Breuer *et al.*, 1975; Wright *et al.*, 2015]. Present work contradicts this observation and shows that the ring-opened isomer formation and the eventual ethylene oxide formation to be dominant. As mentioned in Table 3.4, in addition to the three major pathways several minor pathways emerged in the simulations. This led to the formation of molecules such as vinyl alcohol, 2-oxopropanal, glyoxal, propanedial, etc. The present work clearly demonstrates that performing dynamics simulations is required to understand and interpret experimental data and to establish atomic level reaction mechanisms.

…